Plasmonic Nanocages as Photothermal Transducers for Nanobubble Cancer Therapy

Ioannis H. Karampelas[1], Kai Liu[2] and Edward P. Furlani[1,2]

[1] Dept. of Chemical and Biological Engineering, [2] Dept. of Electrical Engineering,
University at Buffalo SUNY, NY 14260, Office: (716) 645-1194, Fax: (716) 645-3822, efurlani@buffalo.edu

ABSTRACT

Plasmonics is emerging from among the most promising means for generating and controlling thermal energy at the nanoscale. In this approach, metallic nanoparticles are laser heated at plasmon resonant wavelengths that depend on the size, shape and properties of the particles. Key attributes of this method include remote optical activation, nanoscale resolution and efficient photothermal transduction. In this presentation we examine photothermal transduction using laser-pulsed colloidal gold nanocage and nanoframe structures. We explore fundamental aspects of this process using computational models that predict the absorption spectra of the nanoparticles, photothermal transduction at plasmon resonance, heat transfer to the fluid and the dynamics of bubble generation under conditions of superheating. We demonstrate that gold nanocages and nanoframes have a substantial absorption cross-section in the NIR that is essentially independent of orientation. In addition, our thermofluidic analysis indicates that by carefully tuning applied power and pulse duration, the generation of controlled nanobubbles is possible without damaging the nanoparticles. Hence, gold nanocages and nanoframes could offer immediate and very selective therapeutic options when properly uptaken since explosive nanobubbles can cause immediate lysis of targeted cells while preventing damage to nearby healthy tissue due to strong cooperative heating effects.

Keywords: Localized surface plasmon resonance (LSPR), nanocages, nanoframes, photothermal energy conversion, plasmonic-enhanced photothermal energy transfer, LSPR-induced optical absorption, pulsed-laser photothermal heating, photothermal therapy, plasmonic nanobubble cancer treatment

1 INTRODUCTION

During the last several years, there has been a proliferation of research on various transducers for photothermal therapy including organic dyes,[1] metallic nanostructures[2] and carbon based nanomaterials.[3] Among these, there has been an emphasis on gold nanoparticles because these are very well suited for bioapplications since they can be synthesized in various shapes and sizes and coated with a variety of enabling agents.[4-6] Representing a fairly recent advance in the field of nanoparticle synthesis, nanocages and nanoframes can now be readily fabricated using bottom-up techniques.[7, 8] One major advantage of these geometries is its porosity. This property makes nanocages and nanoframes a great candidate for drug encapsulation and optically controlled photothermal drug delivery. [2, 6] Moreover, nanocages have also shown increased potential for a wealth of applications including photothermal treatment,[4] catalysis,[9] optical imaging,[10] cancer diagnosis[11] and photodynamic therapy[12] among others. Some of the most promising areas of interest involves the use of gold nanocages for cancer detection and subsequent photothermal destruction of cancer cells; a process where an increase in the temperature of a colloid of gold nanoparticles, preferably uptaken by cancer cells, is achieved remotely through laser irradiation, thus leading to cell apoptosis or necrosis.[13, 14] However, if such temperature rise is not sufficiently localized there may be unwanted damage to nearby healthy cells. Hence, the need arises to better study the diffusion and control thermal energy at the nanoscale or investigate alternative methods of treatment such as cell membrane lysis through explosive nanobubble nucleation.

Laser-based plasmonic photothermal energy conversion is of particular interest since it allows for highly localized efficient heating. In this approach, illuminating the targeted nanostructures with a pulsed laser at their plasmon resonance frequency can result in optimum energy absorption because of the coherent and collective oscillation of electrons within the nanostructures, resulting in a maximized colloidal heating effect. The plasmon resonance frequency can, in turn, be tuned from the ultraviolet (UV) through the near-infrared (NIR) spectrum by controlling their size and especially their shape during the synthesis process.[15-17]

Thus far, we have used computational models to elucidate the fundamental physics of plasmon-enhanced photothermal transduction for various nanoparticle geometries that exhibit some form of axial symmetry, such as nanorods, nanotori and nanorings.[15, 17] It suffices to use a 2D analysis for these structures because of their axial symmetry. In this presentation, we study the photothermal physics of laser heated plasmonic nanocages and nanoframes, which is more challenging since it requires a full 3D analysis. Through the use of computational models, we are able to investigate the plasmon resonance behavior of the nanoparticles as a function of their geometric aspect ratios and orientation with respect to the incident polarization. We also study their thermofluidic behavior,

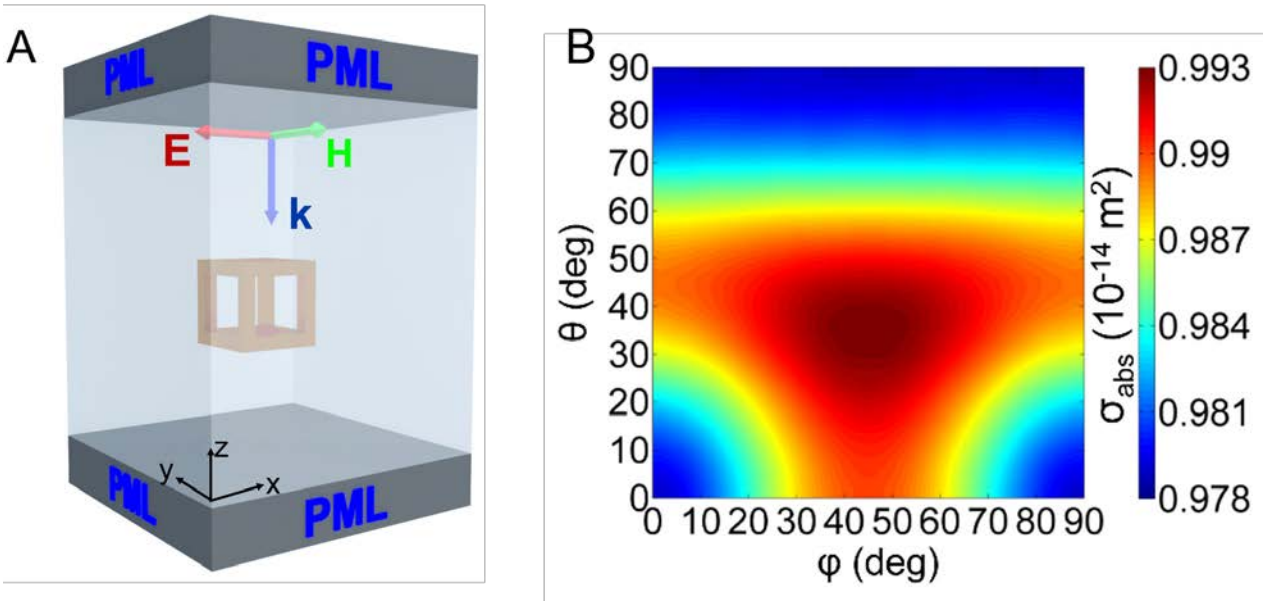

Figure 1. Photonic analysis of an Au nanocage (L=28nm and W=7nm): (a) computational domain (b) optical absorption cross section σ_{abs} vs orientation.

i.e. heat transfer to the fluid and the dynamics of bubble generation under conditions of superheating. For all cases studied, we consider nanosecond-pulsed laser illumination of the nanoparticles in fluid leading to bubble nucleation, wherein the pulse duration exceeds the characteristic time constants for initial non-equilibrium photothermal transient effects. Our results show that randomly oriented nanocages are best suited for colloidal photothermal manifestation due to their higher absorption efficiency. We demonstrate that various nanocage geometries also exhibit a resonance peak in the NIR, which in combination with their high absorption in random orientations, qualify them as exceptional photothermal transducers for deep tumor penetration and photoactivated drug delivery.

2 RESULTS AND DISCUSSION

We model laser-induced plasmon-enhanced photothermal effects using continuum-level photonic and fluidic analysis. We use computational electromagnetics to predict photothermal energy conversion within the nanoparticles, i.e. the time-averaged power absorbed by a particle as a function of the wavelength and polarization of the incident light. Subsequently, the absorbed power is converted into heat and the particle becomes a heat source within the fluid. As the particle heats up, thermal energy is transferred to the fluid and, under illumination of sufficient intensity, a vapor bubble can nucleate at the particle-fluid interface if the critical vaporization temperature of the fluid is reached. Once nucleated, a bubble will exhibit a dynamic behavior (expansion and collapse) that is a complex function of the heat and mass transfer at the bubble-fluid interface as well as the temperature and flow in the surrounding fluid. This simulation is achieved using computational fluid dynamic (CFD) analysis.

2.1 Photonic Simulations

In this section, we perform a theoretical analysis on the optical properties of Au nanocages by using the finite element based radio frequency solver in the COMSOL Multiphysics program. The computational domain is shown in **Figure 1a**. A single Au nanocage is centered at the origin of the domain. The particle is illuminated by a uniform downward-directed plane wave which is linearly polarized along x-axis. Perfectly matched layers (PML) are applied at the top and bottom of the domain to reduce backscatter from these boundaries. Periodic boundary conditions are applied at the boundaries perpendicular to **E** and **H**. The boundary conditions mimic the response of a 2D array of identical nanocage structures with center-to-center x and y lattice spacing equal to the width of the computational domain in the x and y directions, respectively. The lattice spacing is chosen to be large enough so that the resulting predictions will reflect the response of a single isolated particle, i.e. with negligible coupling with neighboring particles. The incident field is generated by a time-harmonic surface current source positioned in the x-y plane directly below the upper PML.

We compute the absorption cross-section σ_{abs} (m^2) of the nanocage as a function of its spatial orientation which is defined by two rotation angles (φ, θ). The absorption cross-section σ_{abs} is calculated from absorbed power (W) divided by the incident irradiance I_{laser} (W/m^2). Since the absorbed energy in the nanocage will be directly converted into the thermal dissipation, σ_{abs} is closely related to the efficiency of the photothermal energy conversion in the particle. Moreover, we define **n** as a vector normal to the top surface of the nanocage. The angle lies in the x-y plane and φ is measured from the x-axis to the projection of **n** onto x-y

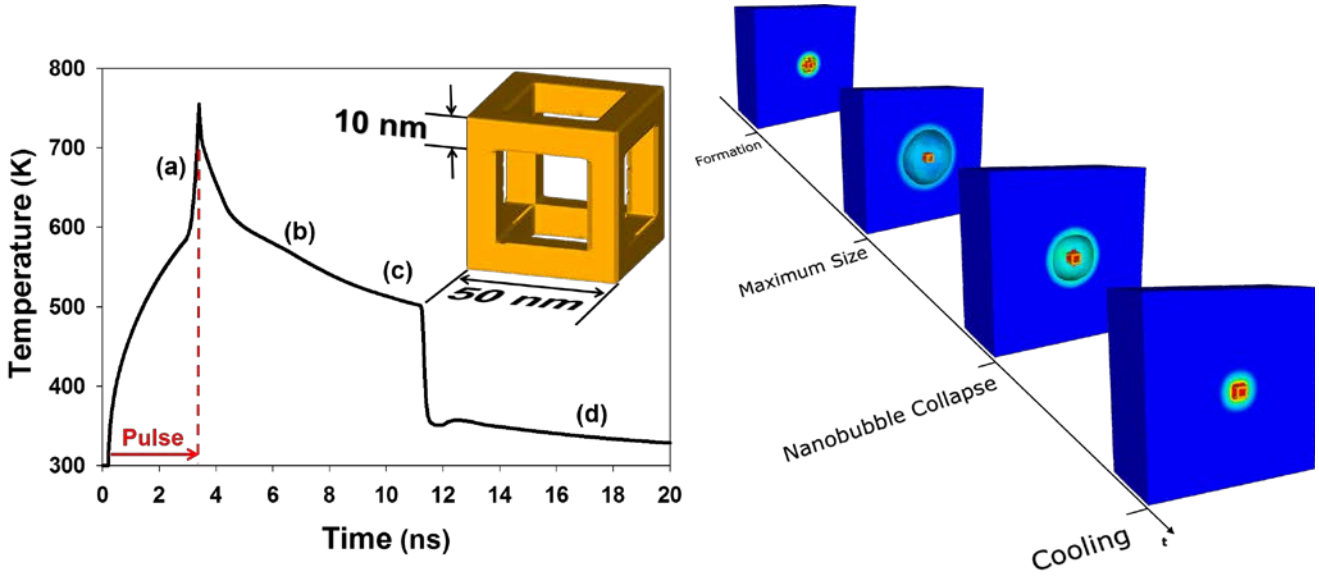

Figure 2. Photothermal heat cycle of a nanocage (L=50nm, W=10nm) (perspective 1/2 view): plot of nanocage temperature vs. time, pulse duration indicated by red arrow and dashed line and inset plots showing various phases of the thermal cycle; (a) nanobubble formation, (b) nanobubble (maximum size), (c) nanobubble collapse, (d) cooling.

plane, while θ is the angle between **n** and z-axis. During our analysis, we found the localized surface plasmon resonance (LSPR) of the Au nanocage strongly depends on the dimensional parameters of the nanocage, i.e. the length L and width W of each edge nanowire. Because of this desirable tunability, we first choose a model with L=28 nm and W=7 nm to realize the LSPR wavelength of 830 nm which falls into the well-defined "therapeutic window". In this window, light penetrates deeper into tissues with less absorption and scattering than at other wavelengths.

We investigate LSPR absorption of the nanocage as a function of its orientation with respect to the polarization of the incident light. This is important for applications involving colloids where nanocages have random orientations within a carrier fluid. The absorption cross section σ_{abs} of the nanocage is plotted in **Figure 1b**. We observed very little variation in σ_{abs} throughout the entire range of orientations. This is desirable for applications such as photothermal cancer therapy as it implied a higher heating efficiency for a given laser irradiance.

2.2 Fluidic Simulations

A 3D CFD analysis was implemented in order to ascertain the pulse duration and power necessary for the nucleation of an explosive nanobubble without causing potential damage to the nanostructures. Due to its symmetry, it sufficed to model one octant of the nanocage.

The fluidic analysis can be divided into two phases. In the first phase, a thermal analysis was performed to predict the power level required to heat a nanocage with an edge length of 50nm and an edge thickness of 10nm from an ambient temperature of 300K to the superheat temperature of water i.e. 580K. This depends on the pulse intensity and duration, which was constrained to be between 3 to 5 ns. In the second phase of the analysis, we applied the power levels obtained in phase one and slightly increased the pulse duration so that the nanoparticles were heated beyond the superheat temperature, which caused vaporization of the surrounding fluid and bubble nucleation. The pulse duration was tuned so that the nanoparticle achieved a temperature that was sufficiently high to generate a sustained nanobubble, but low enough (< 1100K) to avoid melting the nanoparticle. Based on our analysis, it was found that a power of 200μW with pulse duration of 3.2ns is adequate for nucleation. The results of the thermo-fluidic analysis are shown in **Fig. 2**.

The nanocage and the fluid are initialized at a temperature of 300K. After 0.2 ns, a heat pulse caused by laser illumination result in a sudden rise in the temperature of the nanoparticle, which is indicated in the temperature vs. time plot of **Fig. 2**. When the nanocage reaches the superheat temperature, a homogeneous water vapor bubble is nucleated around it. Upon nucleation, the temperature of the nanoparticle rises rapidly since it is being insulated by a thin sheath of vapor while still being heated. This continues until the end of the heat pulse, which coincides with the bubble formation and maximum temperature as shown in plot segment and inset figure (a). The pulse duration is 3.2ns as indicated by the red dashed line. After it is nucleated the nanobubble expands because of its higher pressure compared to the surrounding fluid. The nanobubble reaches a maximum size as shown in inset figure (b). For this geometry, the maximum bubble radius achieved was 185nm. Eventually, the nanobubble collapses bringing fluid back in contact with the nanoparticle as shown in plot segment and inset figure (c), gradually reducing its temperature to the ambient temperature (d). An

interesting observation of this process is the formation of a hot droplet of fluid in the middle of the nanoparticle, which partially evaporates as the nanobubble expands. The CFD simulation was performed on a 12-core workstation with 128 GB of RAM. The time for the simulation was approximately 200 hours.

3 CONCLUSIONS

We have used a combination of computational electromagnetic and fluid dynamic analysis to study the effects of nanosecond-pulsed laser heating of Au nanocages and nanoframes. Our results demonstrate that such nanostructures exhibit a much higher absorption (photothermal transduction) over a wide range of orientations with respect to the incident polarization as compared to other nanoparticles with less 3D symmetry such as nanorods. Nanocages have high average absorption for random orientations and, therefore, Au nanocage structures are well-suited as photothermal transducers and hold promise for photothermal therapy. Our modeling approach can be used to explore fundamental behavior of nanoscale photothermal processes and is useful for the rational design of novel plasmonic structures for a wide range of applications.

REFERENCES

1. Zheng, X.H., et al., *Enhanced Tumor Treatment Using Biofunctional Indocyanine Green-Containing Nanostructure by Intratumoral or Intravenous Injection.* Molecular Pharmaceutics, 2012. **9**(3): p. 514-522.
2. Khlebtsov, N., et al., *Analytical and Theranostic Applications of Gold Nanoparticles and Multifunctional Nanocomposites.* Theranostics, 2013. **3**(3): p. 167-180.
3. Moon, H.K., S.H. Lee, and H.C. Choi, *In Vivo Near-Infrared Mediated Tumor Destruction by Photothermal Effect of Carbon Nanotubes.* Acs Nano, 2009. **3**(11): p. 3707-3713.
4. Chen, J.Y., et al., *Gold Nanocages as Photothermal Transducers for Cancer Treatment.* Small, 2010. **6**(7): p. 811-817.
5. Skrabalak, S.E., et al., *Gold nanocages for biomedical applications.* Advanced Materials, 2007. **19**(20): p. 3177-3184.
6. Yavuz, M.S., et al., *Gold nanocages covered by smart polymers for controlled release with near-infrared light.* Nature Materials, 2009. **8**(12): p. 935-939.
7. Sun, Y.G. and Y.N. Xia, *Alloying and dealloying processes involved in the preparation of metal nanoshells through a galvanic replacement reaction.* Nano Letters, 2003. **3**(11): p. 1569-1572.
8. Wan, D., et al., *Robust synthesis of gold cubic nanoframes through a combination of galvanic replacement, gold deposition, and silver dealloying.* Small, 2013. **9**(18): p. 3111-3117.
9. Zeng, J., et al., *A comparison study of the catalytic properties of Au-based nanocages, nanoboxes, and nanoparticles.* Nano letters, 2009. **10**(1): p. 30-35.
10. Cang, H., et al., *Gold nanocages as contrast agents for spectroscopic optical coherence tomography.* Optics letters, 2005. **30**(22): p. 3048-3050.
11. Kim, C., et al., *In vivo molecular photoacoustic tomography of melanomas targeted by bioconjugated gold nanocages.* ACS nano, 2010. **4**(8): p. 4559-4564.
12. Gao, L., et al., *Hypocrellin-loaded gold nanocages with high two-photon efficiency for photothermal/photodynamic cancer therapy in vitro.* Acs Nano, 2012. **6**(9): p. 8030-8040.
13. Pitsillides, C.M., et al., *Selective cell targeting with light-absorbing microparticles and nanoparticles.* Biophysical journal, 2003. **84**(6): p. 4023-4032.
14. West, J.L. and N.J. Halas, *Engineered nanomaterials for biophotonics applications: improving sensing, imaging, and therapeutics.* Annual Review of Biomedical Engineering, 2003. **5**(1): p. 285-292.
15. Alali, F., et al., *Photonic and Thermofluidic Analysis of Colloidal Plasmonic Nanorings and Nanotori for Pulsed-Laser Photothermal Applications.* Journal of Physical Chemistry C, 2013. **117**(39): p. 20178-20185.
16. Frangioni, J.V., *In vivo near-infrared fluorescence imaging.* Current Opinion in Chemical Biology, 2003. **7**(5): p. 626-634.
17. Furlani, E.P., I.H. Karampelas, and Q. Xie, *Analysis of pulsed laser plasmon-assisted photothermal heating and bubble generation at the nanoscale.* Lab on a Chip, 2012. **12**(19): p. 3707-3719.